Figure S1. Summertime **(a)** surface and **(b)** column concentrations of OA in the SEUS. Color shades represent OA components from each scheme. In attached text, "m" represents 2000-2016 relative trend with units of %/year; numbers in parenthesis in (a) and (b) represent trends with units of $\mu g/m^3$/year or mg/m^2/year; "avg" represents the 17-year average with units of $\mu g/m^3$ in (a) and mg/m^2 in (b).
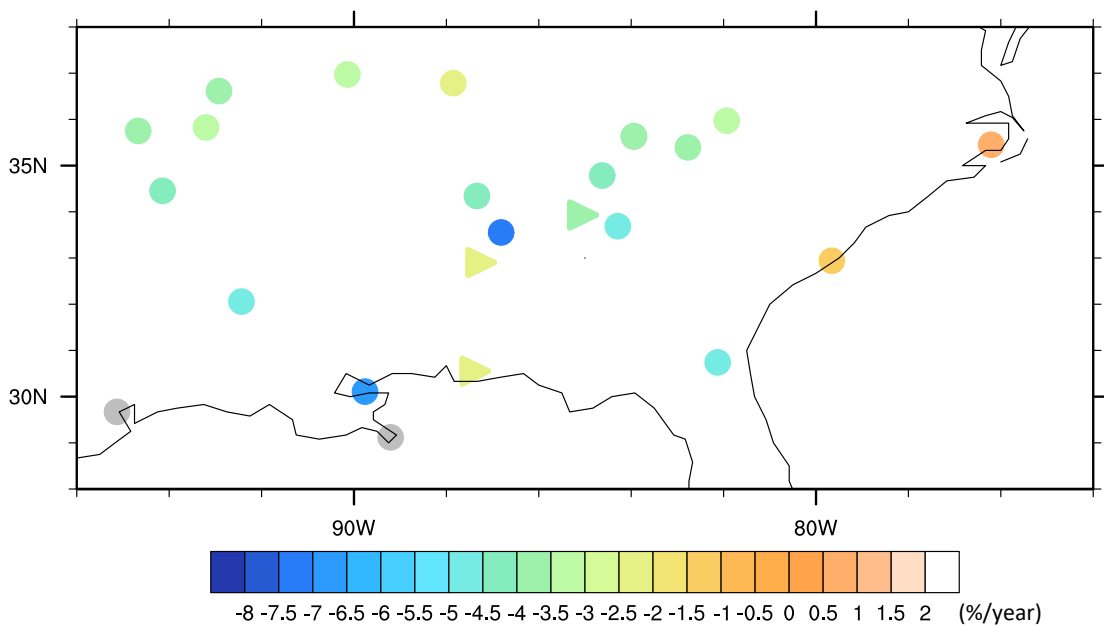
Figure S2. Relative trend of OA (units: %/year) for each site from the IMPROVE (circle) and SEARCH (triangle) networks. Grey points represent sites which have less than 5 years' data.
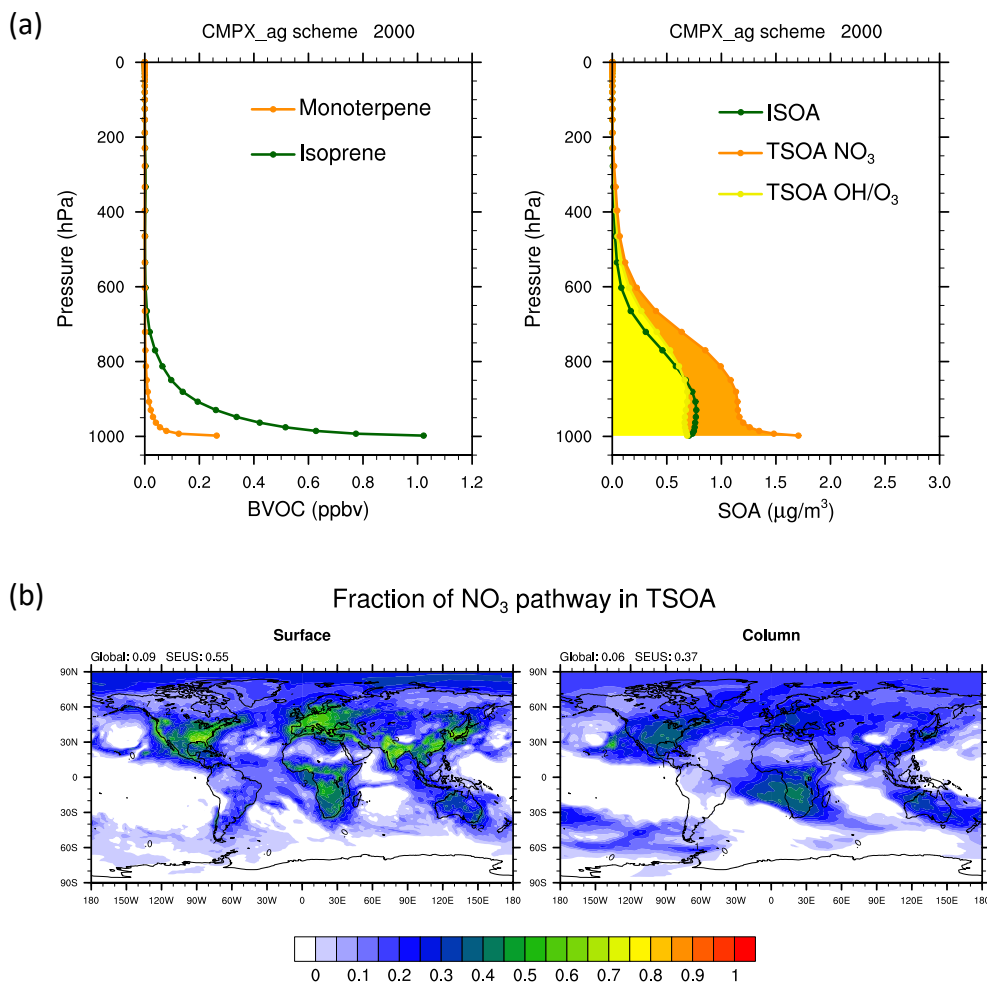
Figure S3. (a) Vertical profile of isoprene, monoterpene, ISOA and TSOA concentrations in the SEUS, and (b) fraction of the NO_3-pathway in TSOA surface and column concentrations in a 1-year test run in 2000 using CMPX_ag. TSOA formed by NO_3-oxidation is determined by the difference between the CMPX_ag simulation and a sensitivity run that turns off the NO_3-pathway.
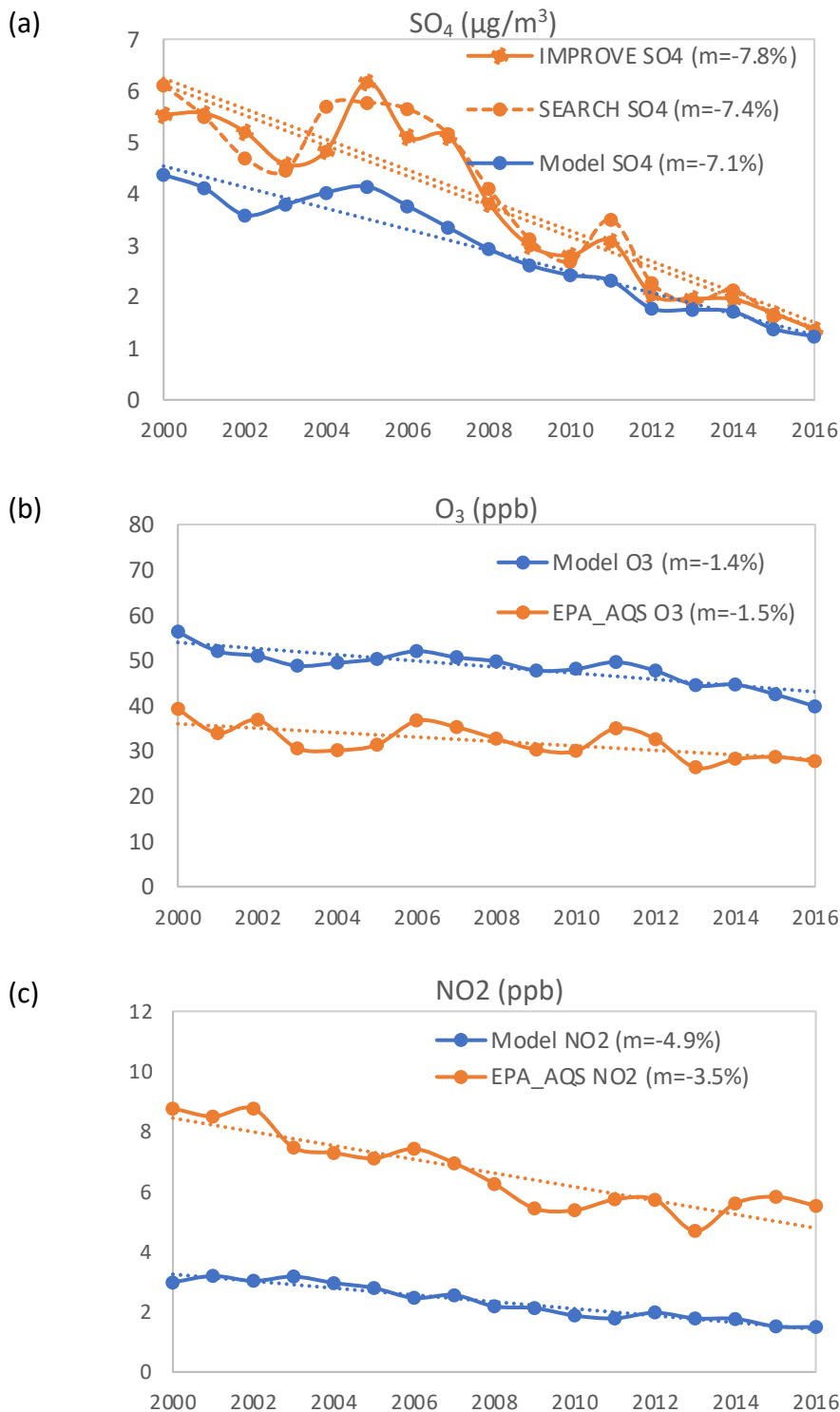
Figure S4. Summertime modeled and measured surface **(a) sulfate** ($\mu g/m^3$) and **(b) O$_3$** (ppb) and **(c) NO$_2$** (ppb) concentrations in the SEUS. Changing rates m have units of % per year relative to their 2000-2016 averages. Model results are from the CMPX_ag scheme. Sulfate measurements are from IMPROVE and SEARCH. O$_3$ and NO$_2$ measurements are from EPA's Air Quality System (https://aqs.epa.gov/aqsweb/airdata/download_files.html).
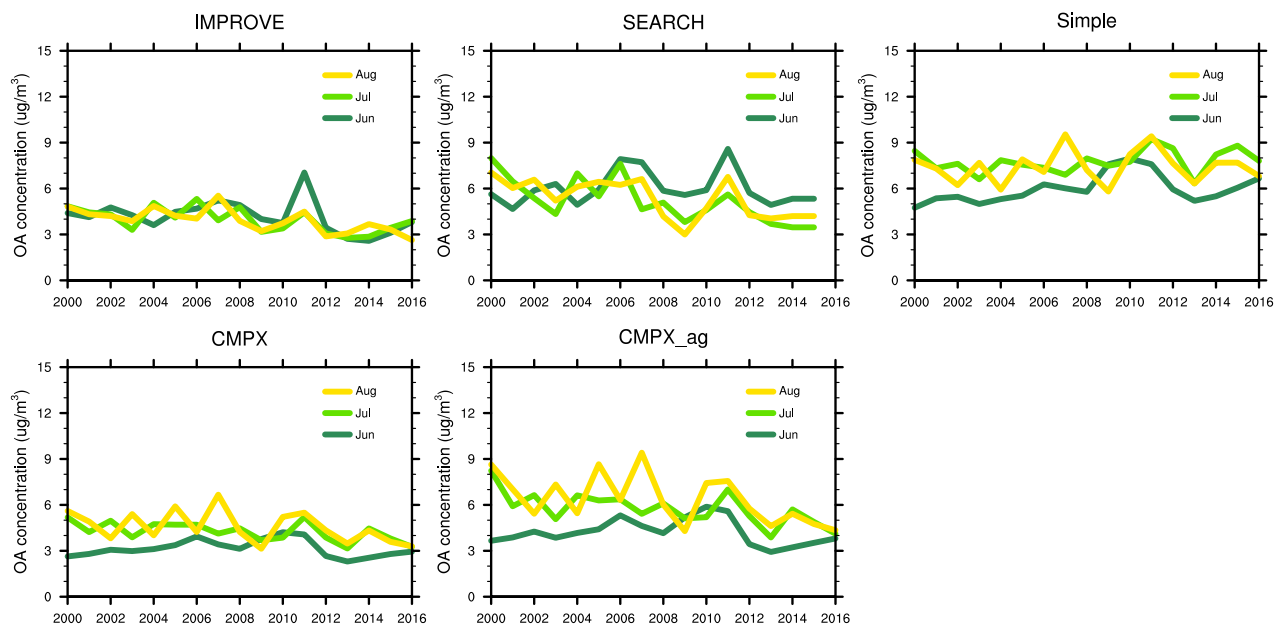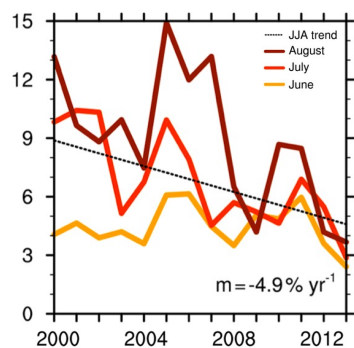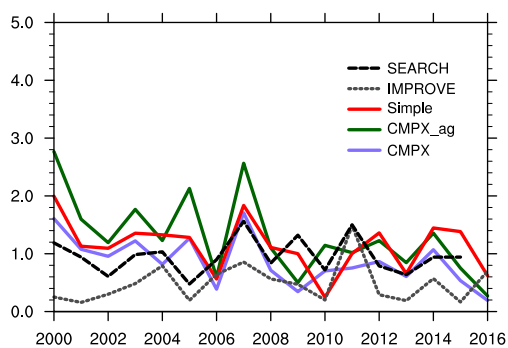
Figure S5. Summertime monthly surface OA (µg/m^3) in the SEUS from **(a)** IMPROVE, SEARCH and all GFDL AM4.1 simulations; and **(b)** from GEOS-Chem v12.1.1. (b) is adapted from Zheng et al. (2020). **(c)** The standard deviation of surface OA (µg/m^3) among June, July and August in the SEUS from IMPROVE, SEARCH, and all GFDL AM4.1 simulations.
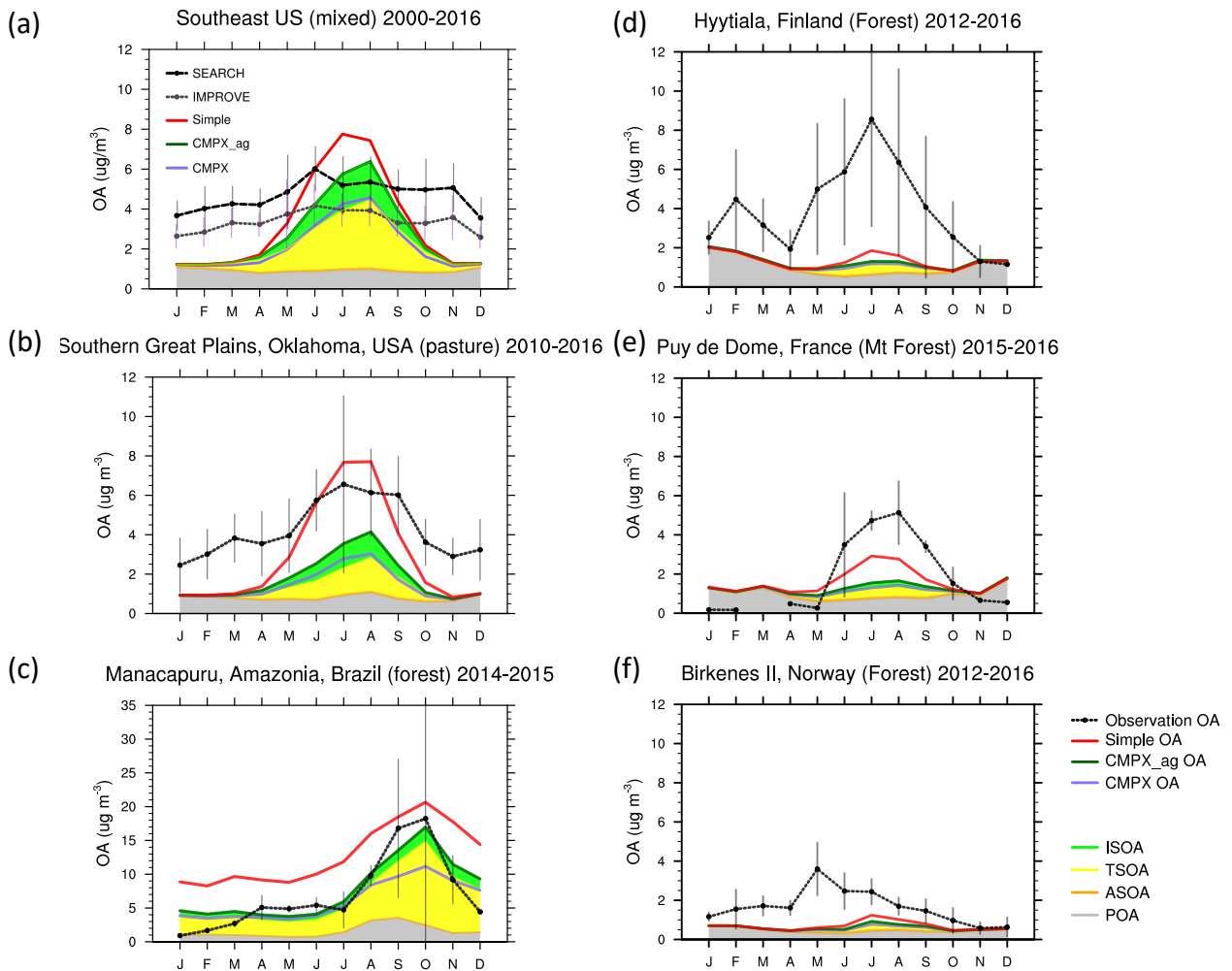
Figure S6. Seasonal cycle of surface OA concentration. Color shades represent OA components from the CMPX_ag scheme. In (a), black and purple dash lines represent filter measurement of OA from the SEARCH and IMPROVE networks. In other figures, black dash lines represent ACSM measurement of OA from the ARM network in (b)~(c) and from the ACTRIS network in (d)~(f).
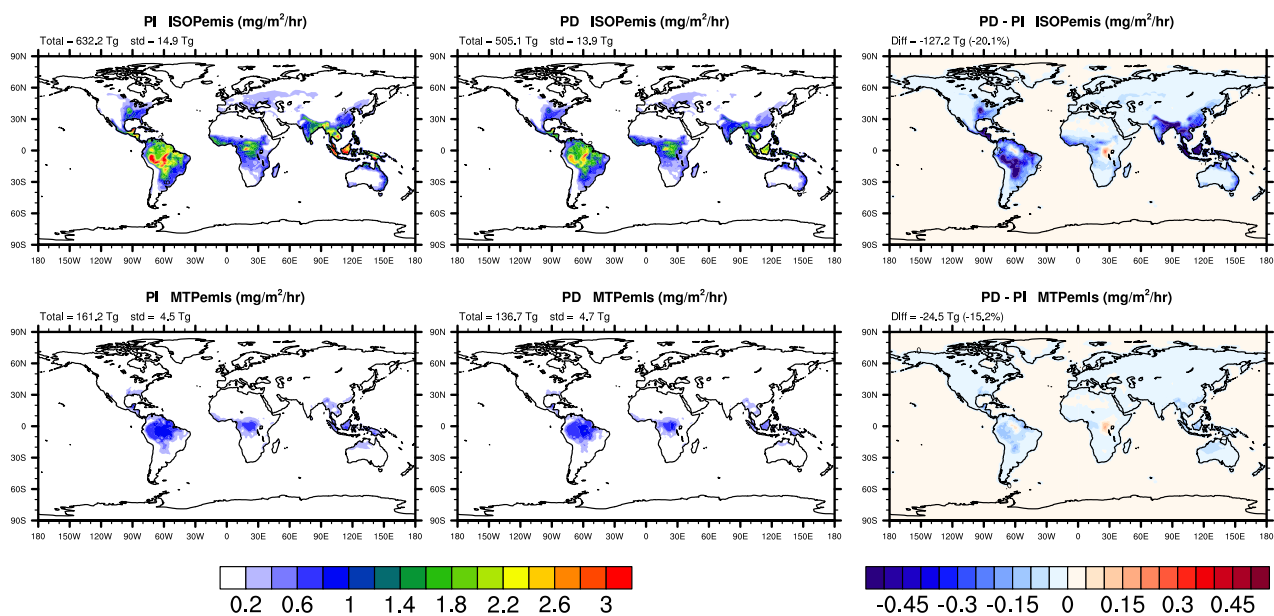
Figure S7. Annual mean isoprene (ISOP) and monoterpene (MTP) emissions (mg/m^2/hour) at pre-industrial (PI) and present day (PD) and their difference. The global total emissions (Tg/year) are listed at the top left of each panel. The BVOC emissions using the Simple, CMPX, and CMPX_ag schemes are similar.
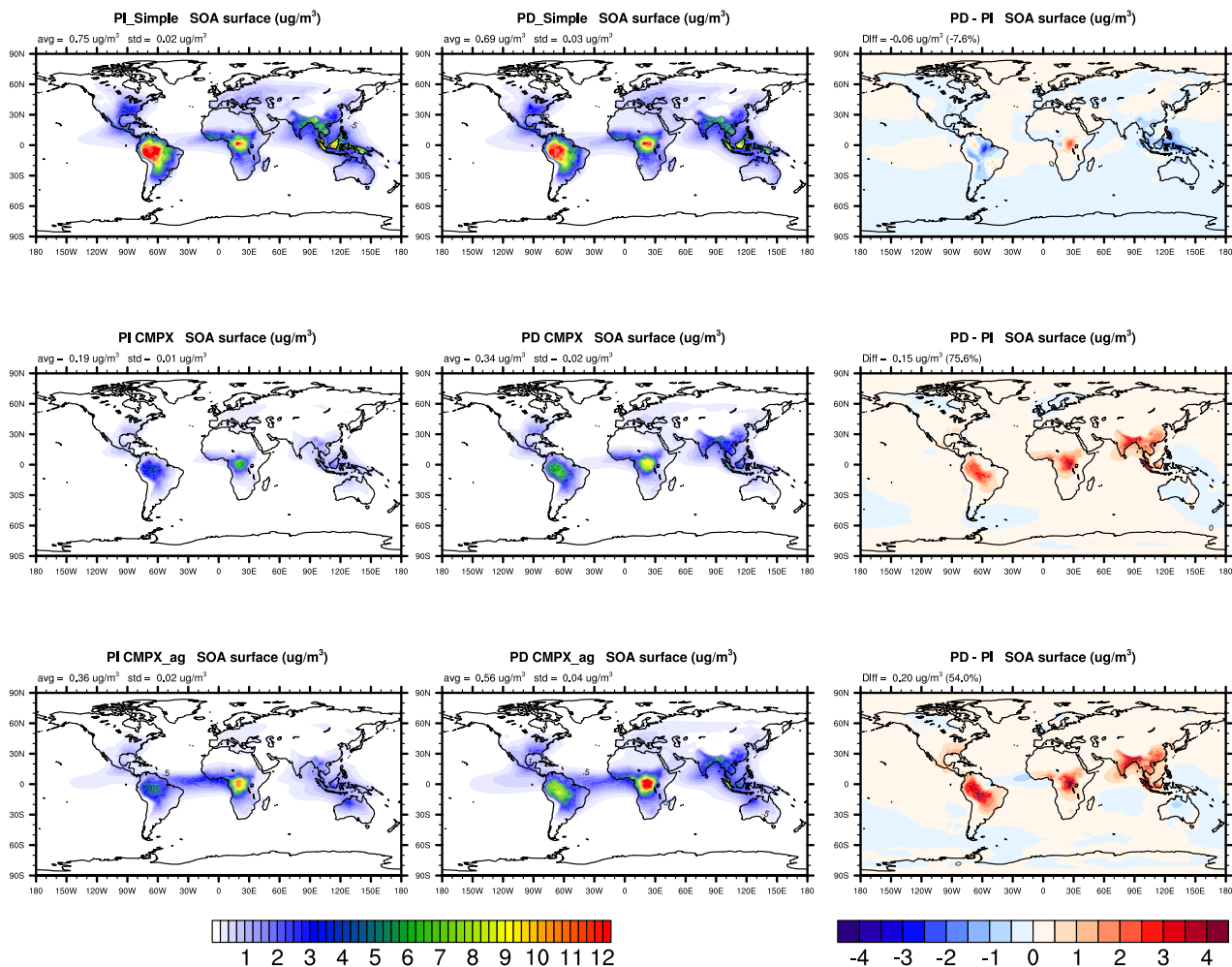
Figure S8. Annual mean ASOA, ISOA and TSOA surface concentration (μg/m³) using the Simple, CMPX and CMPX_ag schemes at pre-industrial (PI) and present day (PD) and their difference. ASOA concentrations in all schemes are similar.
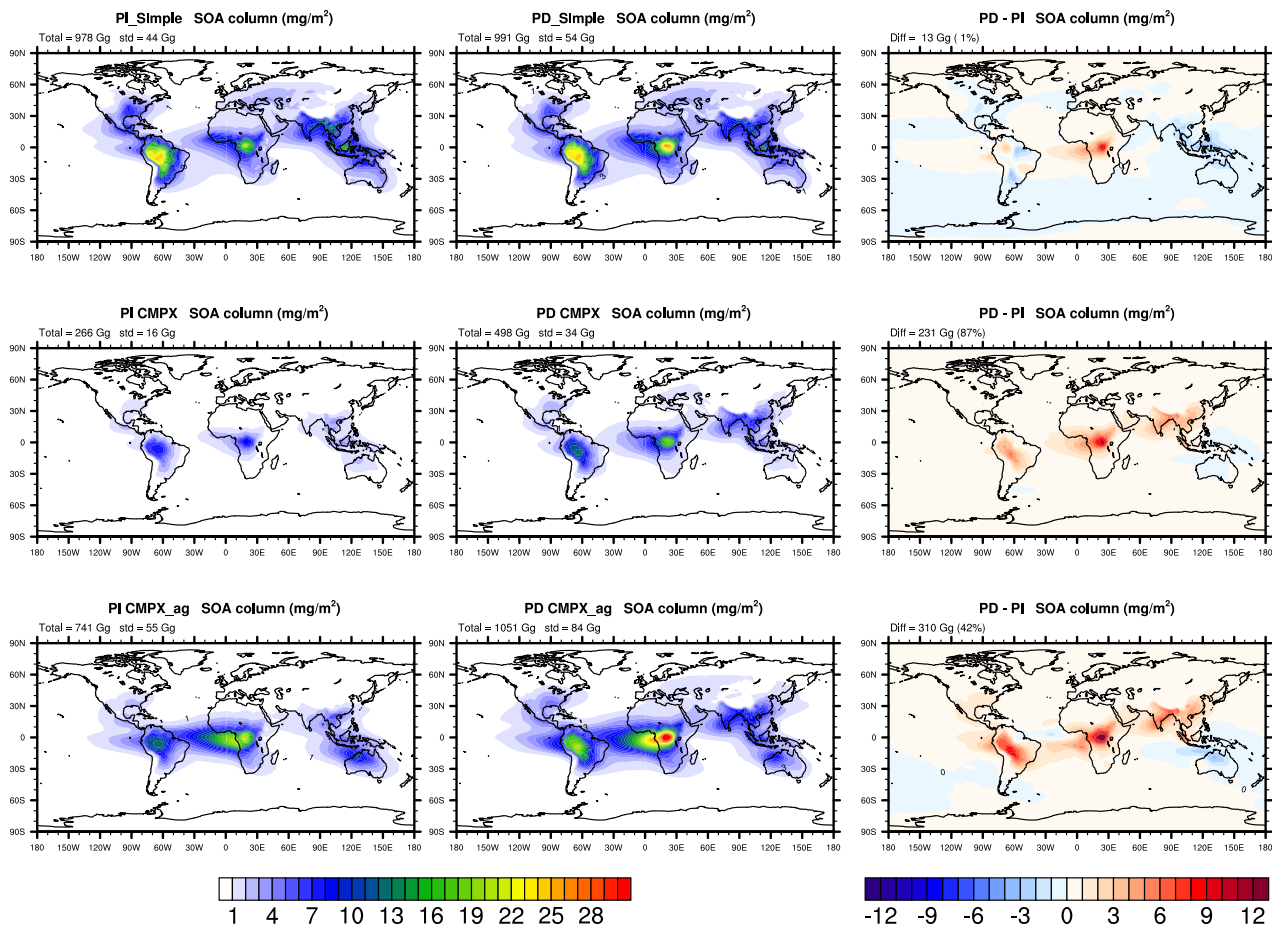
Figure S9. Annual mean SOA column concentration (mg/m^2) using the Simple, CMPX and CMPX_ag schemes at pre-industrial (PI) and present day (PD) and their difference. The global burden (Gg) are listed at the top left of each panel.
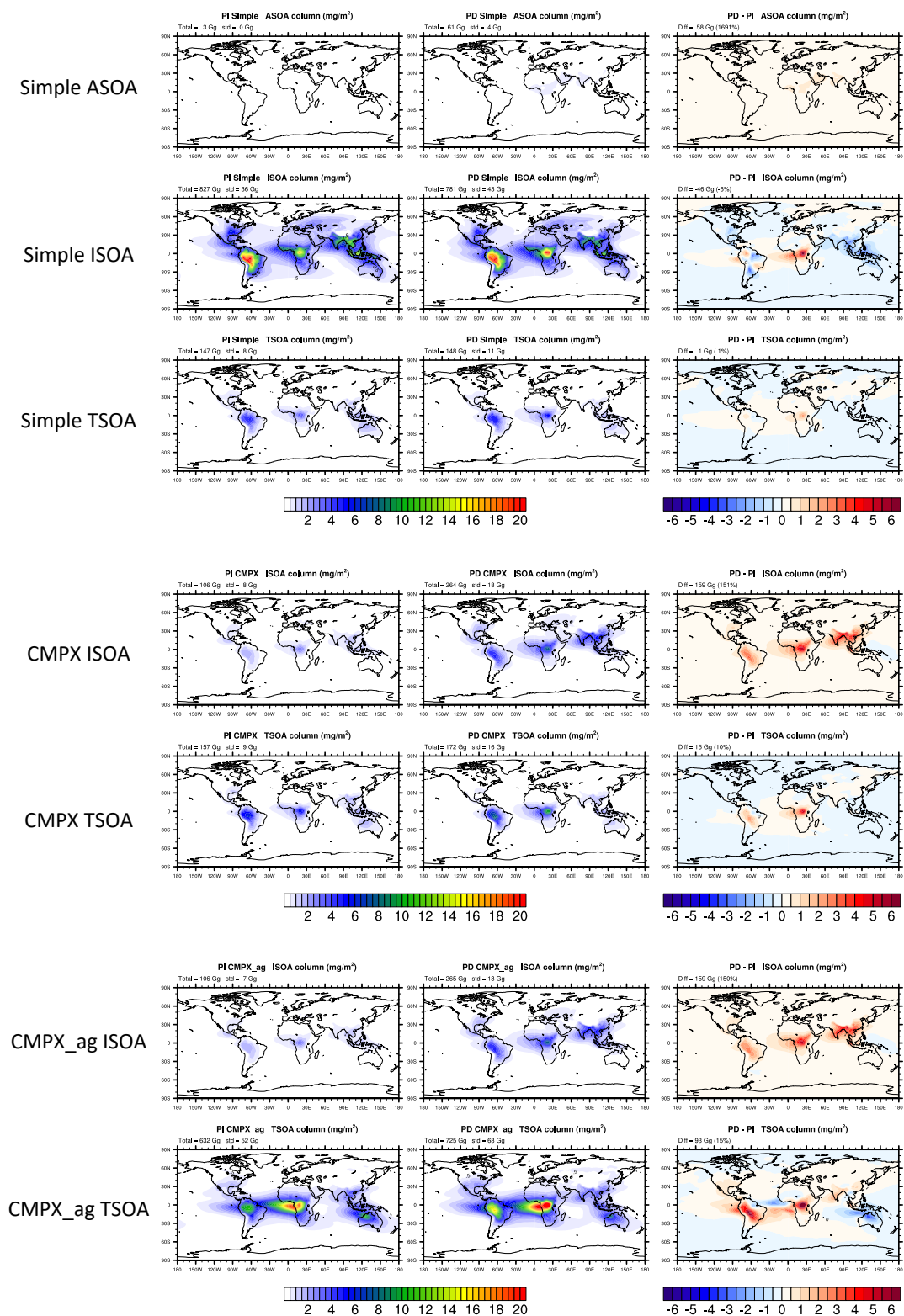
Figure S10. Annual mean ASOA, ISOA and TSOA column concentration (mg/m^2) using the Simple, CMPX and CMPX_ag schemes at pre-industrial (PI) and present day (PD) and their difference. The global burden (Gg) are listed at the top left of each panel. ASOA is similar among different schemes.
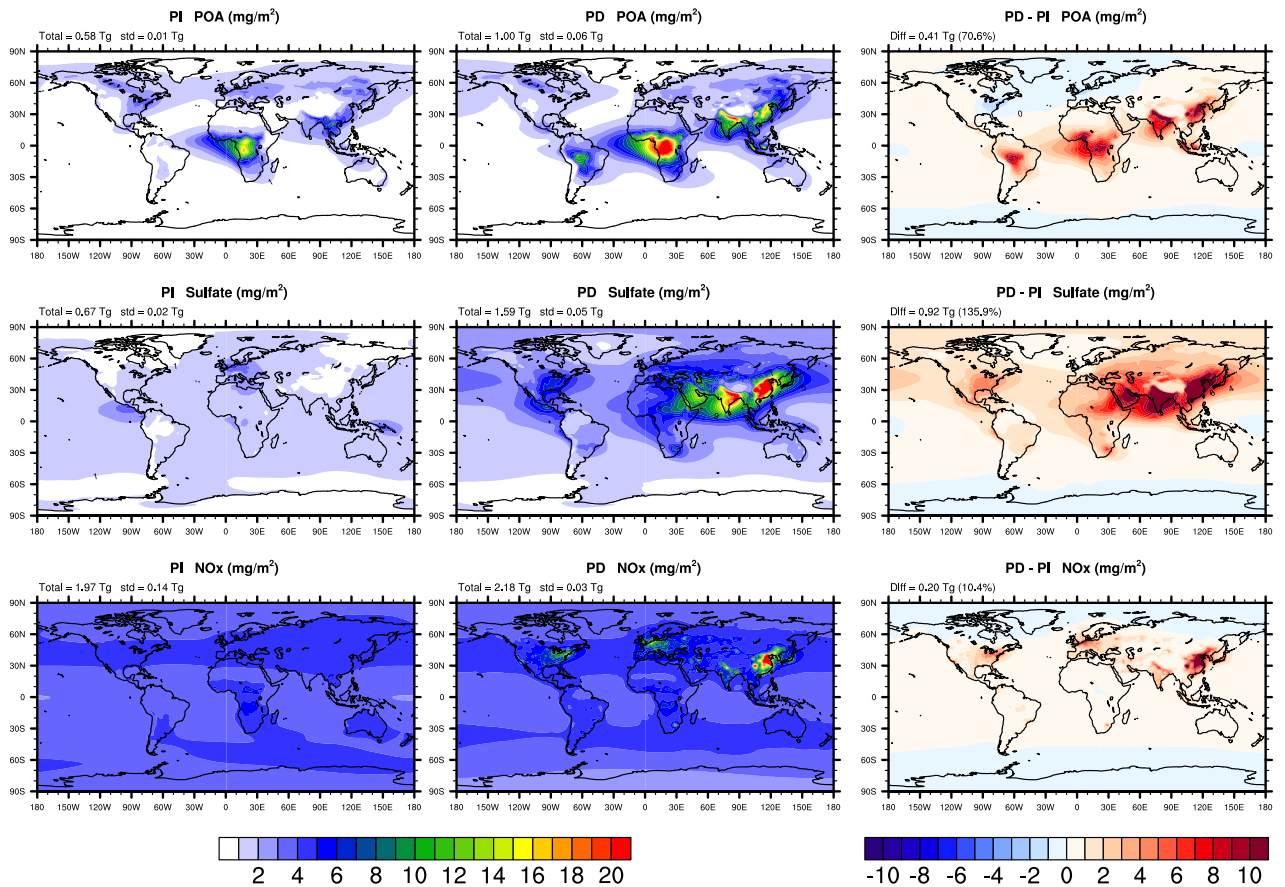
Figure S11. Annual average column concentrations (in units of mg/m^2) of POA, sulfate aerosol and NO$_x$ at pre-industrial (left column) and present-day (middle column) and their differences (right column). Their global burdens (in units of Tg) are listed on the top left of each panel.
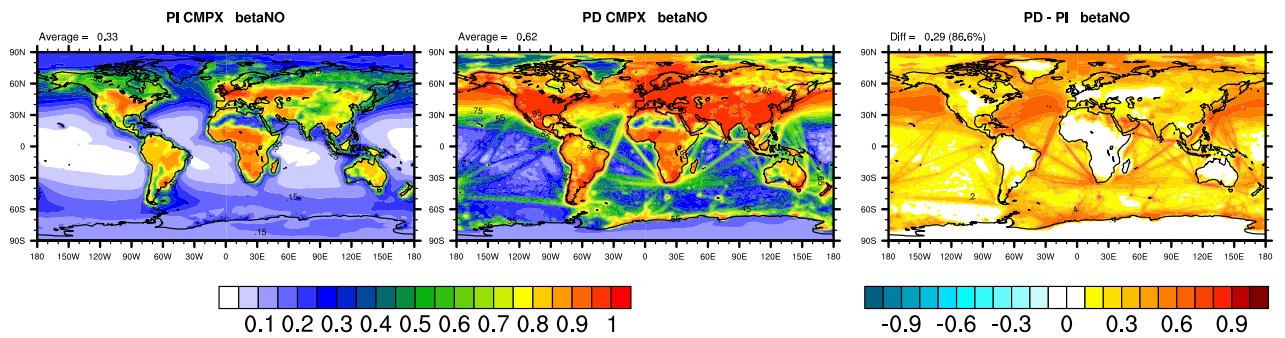
Figure S12. Annual mean branching ratio (betaNO) at pre-industrial (left column) and present-day (middle column) and their differences (right column). Their global averages are listed on the top left of each panel.
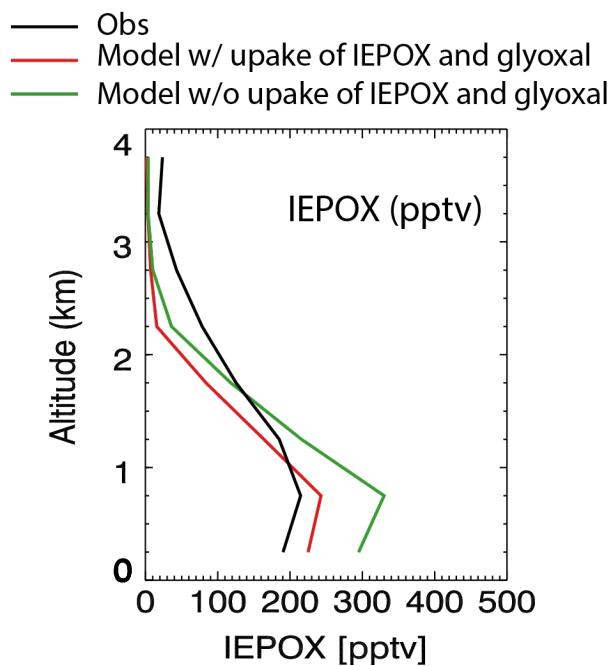
Figure S13. Mean vertical profile of IEPOX during the NASA SEAC[4]RS (Studies of Emissions, Atmospheric Composition, Clouds and Climate Coupling by Regional Surveys) aircraft campaign. Measurements are shown in black, and two model simulations (using a previous version AM3) with and without aerosol reactive uptake of IEPOX and glyoxal using uptake coefficients of 0.001 are shown in red and green lines, respectively.